


Article

Optimal Energy Integration and Off-Design Analysis of an Amine-Based Natural Gas Sweetening Unit

Amine Berchiche^{1,2,3,*}, Mohamed Guenoune³, Salah Belaadi² and Grégoire Léonard¹ ¹ Department of Chemical Engineering, Université de Liège, B6a Sart-Tilman, 4000 Liège, Belgium² Laboratory of Reaction Engineering, Université des Sciences et de la Technologie Houari Boumediene, BP32 El-Alia, Algiers 16000, Algeria³ Algerian Petroleum Institute, Sonatrach, 1st Novembre Street, Boumerdes 35000, Algeria

* Correspondence: mea.berchiche@uliege.be

Abstract: The present paper focuses on the efficiency enhancement of the energy-intensive natural gas (NG) sweetening process in the context of upstream natural gas production. A bi-level heat integration scheme is proposed including direct recycling of available high-temperature waste heat and harnessing the excess low-temperature waste heat in an optimized organic Rankine cycle (ORC) for power production. The energy performance of the whole model was studied under a range of possible reservoir conditions. A particle swarm optimization (PSO) algorithm was adopted to simultaneously optimize the parameters of the heat recovery network as well as the ORC cycle parameters. Finally, in order to account for the impact of perturbations of the heat source and sink, an off-design performance analysis was conducted using real-time data from an industrial plant. The proposed integration methodology was found to be effective across most of the reservoir conditions covered in this study. At optimal integration, a reduction of 40% up to 100% in heating requirements of the amine process was reported, as well as a net electricity production of 30% up to 190% of the electrical demand of the background process. The use of propane (R290) as a working fluid resulted in the highest energy output, whereas higher carbon number fluids allowed a better energy/working pressure trade-off. The off-design analysis allowed for the quantification of the impact of operational fluctuations of the background process on integration performance. Energy savings resulting from direct heat integration were found to range from 68% up to 103% of the expected design value, whereas the ORC net energy output respective to the use of R290, R600a, and R601a was found to range from 60% to 132%, 47% to 142%, and 52% to 135%.

Keywords: carbon capture; decarbonization of natural gas industry; process integration; particle swarm optimization; organic Rankine cycle



Citation: Berchiche, A.; Guenoune, M.; Belaadi, S.; Léonard, G. Optimal Energy Integration and Off-Design Analysis of an Amine-Based Natural Gas Sweetening Unit. *Appl. Sci.* **2023**, *13*, 6559. <https://doi.org/10.3390/app13116559>

Academic Editors: Grazia Leonzio and Filippo Bisotti

Received: 10 April 2023

Revised: 13 May 2023

Accepted: 25 May 2023

Published: 28 May 2023



Copyright: © 2023 by the authors. Licensee MDPI, Basel, Switzerland. This article is an open access article distributed under the terms and conditions of the Creative Commons Attribution (CC BY) license (<https://creativecommons.org/licenses/by/4.0/>).

1. Introduction

In recent years, environmental awareness and stringent regulations have pushed many industrial sectors to explore alternative sources of energy as well as efficient technologies for its conversion. Driven by its high-energy intensity and low emission rate compared to other fossil fuels, natural gas is playing the role of a bridge fuel to complement the renewable-based global energy mix. Natural gas currently accounts for 25% of the global primary energy consumption, and its global demand is forecasted to increase by 30% between 2020 and 2050 [1,2]. However, despite its advantages, the natural gas value chain is impacted by its high energy consumption and the large amounts of waste heat generated along its production and processing that are discharged into the atmosphere. Recovering and converting this wasted energy into useful work can result in considerable economic savings and alleviate the energy burden of the natural gas industry.

Waste heat is estimated to represent 20% to 50% of industrial energy consumption, 50% of which is difficult to harness due to its low temperature [3]. As a result, several

technologies were investigated in the literature for both high-grade and low-grade waste heat recovery in industrial processes, such as direct heat integration, organic Rankine cycles, Kalina cycles, heat pumps, and absorption chillers, among others [4]. Direct heat integration (DHI) is the most efficient way for the recovery of high-grade waste heat in industrial processes. On another hand, the organic Rankine cycle (ORC) allows the recovery of low-grade waste heat and presents many advantages over other thermodynamic cycles such as simplicity in terms of design and implementation, reliability, and moderate operating conditions [5], which promote this technology as a suitable candidate for low-grade waste heat recovery. In recent years, ORC has found applications in many industrial sectors including glass, cement, geothermal, and solar-based processes with a power output ranging from 10 kW to 20 MW [6]. DHI and ORC applications in the energy-intensive oil and gas sector have also attracted research attention; several papers discussed advanced integration strategies for NG processing units based on heat exchanger networks. Shaikh et al. [7] proposed the integration of dehydration and condensate stabilization units, whereas Zhang et al. investigated the simultaneous optimization of the design parameters and heat integration for NG purification units [8]. Moreover, Yu et al. [9] focused on using ORC as a waste heat recovery method from multiple streams in oil refineries, whereas Veloso et al. [10] investigated the use of ORC to enhance the energy efficiency of offshore oil production facilities. Similarly, in the natural gas industry, Hi and Lin [11] examined the integration of waste heat from natural gas liquefaction turbines with an optimized ORC. Zhao et al. [12] integrated a two-stage ORC to recover cold energy from natural gas regasification units, whereas Bianchi et al. [13] investigated the feasibility of ORC integration in natural gas compression stations. In contrast to down- and midstream natural gas processing, which have been thoroughly studied in the literature, we have noticed that the impact of using ORC integration in the upstream processing of natural gas is scarcely cited.

As presented in Figure 1, the upstream processing of natural gas consists of primary compression, elimination of impurities such as Mercury, CO₂, and H₂O from the raw feed, and primary separation in order to meet transport specifications. Among these steps, CO₂ removal, known as natural gas sweetening and which is based on solvent absorption/regeneration, was found to feature the highest energy demand. In fact, several improvement routes have been proposed in the literature for this process in order to alleviate its high energy intensity, such as the development of new solvents with reduced regeneration requirements, advanced process configurations, and the optimization of plant operating parameters using process simulation tools [14,15].

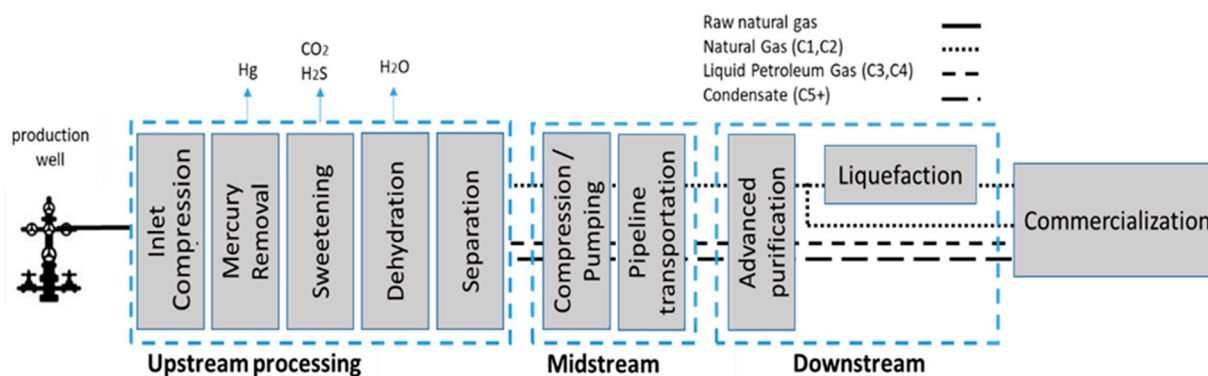


Figure 1. Overview of the overall natural gas processing chain.

In this paper, we have investigated the optimal use of waste heat from the upstream conditioning of natural gas as a solution for energy efficiency enhancement. The quality and quantity of available waste heat were evaluated for sixteen (16) different scenarios, and then a bi-level approach combining DHI and ORC was adopted to investigate the impact of using both high-grade and low-grade waste heat in each scenario.

2. Energy Assessment of the Background Process

Data collected from three different natural gas upstream production facilities operated by the Algerian national oil company, Sonatrach, were analyzed in order to assess the energy demand in the upstream processing chain and identify the units with the highest potential for integration. Energy demand as well as the quality and quantity of waste heat from each unit are presented in Table 1. Due to confidentiality concerns, heating requirements and waste heat quantity are presented as a ratio to the sweetening unit.

Table 1. Energy assessment of the main parts of NG upstream processing chain.

		Compression	Sweetening	Dehydration	Separation
Technology		Turbine-driven	Amine based	Adsorption	Expander
Temp. requirements	°C	NA	127	260	220
Heating requirements	(-)	NA	1.00	0.43	0.91
Waste heat quant.	(-)	3.28	1.00	0.72	0.94
Waste heat quality	°C	131–500	70–89	260–265	40–60

The results show that the amine-sweetening unit features the highest thermal energy demand within the NG processing chain. This observation matches many research papers concluding that despite its maturity and large utilization, high energy intensity has always been reported as a major drawback of amine-based sweetening units [16]. On the other hand, the analysis revealed that the turbine-driven NG compression unit is associated with the highest quantity and quality of waste heat because of its high power demand as well as its inherent low energy conversion efficiency. Table 1 also indicates that the amount of waste heat available from the compression step is available at a higher temperature than the amine unit's requirement. Consequently, heat and process integration emerges as an appropriate solution to bridge the energy efficiency gap in the upstream processing of natural gas, and the compression/amine-based sweetening units are the ideal candidates for this integration. These units were set to be the scope of our study and are considered as the background process.

The inlet natural gas compression process is a crucial step in the processing chain as it maintains a stable plant pressure over the years of production by compensating for the natural decrease in reservoir pressure. On the other hand, the amine-based NG sweetening process, which is equally important, reduces the CO₂ content in order to meet the transport specification, i.e., less than 2 mol-%.

The available data collected from industry are restricted to a narrow range of reservoir pressures and CO₂ contents. Therefore, in order to study the potential of the proposed integration over a wider range of conditions, AspenHysys V11 was used to build a model of the targeted processes, which includes a turbine-driven compression station and an amine-based sweetening unit. MDEA/DEA was selected as the working solvent for this study because of the advantages it presents such as stability and high absorption capacity. The operating pressure of the absorber and regenerator was set to 80 bar and 2 bar, respectively. A feed of 10 MMSCM/Day of sour natural gas was considered for this study, with sixteen scenarios spanning a range of CO₂ molar content from 4 to 10 mol-% and an admission pressure at the turbine inlet ranging from 30 to 60 bar, which corresponds to compression ratios ranging from 2.66 to 1.33.

The compression unit considered in this study is turbine-driven using natural gas as a fuel. It was modeled using the Peng–Robinson equation of state [17] and was validated against data from Siemens SGT series openly provided by the manufacturer [18]. The estimated overall efficiency of the turbine-driven compressor as well as the exhaust gas flow rate was compared to manufacturer data, and a deviation of less than 2% was observed for both factors. On the other hand, the amine unit was modeled using an equilibrium approach based on the Li–Mather empirical model [15,19] and was then validated against industrial data. The predicted CO₂ content in sweet gas, reboiler duty, and temperature

profiles in both absorber and regeneration columns showed a deviation of less than 5% compared to real plant data.

The developed models were used to generate a mapping of energy demand as well as waste heat quantity and quality of the background process across the entire investigation ranges. The targeted process features four sources of waste heat and one heat utilization point, the properties of which are summarized in Table 2. Results showed that the temperature of the hot streams depends on the modeled case. For instance, the turbine exhaust will vary from 550 °C for a compression ratio of 2.66 bar down to 502 °C at a compression ratio of 1.33, and the corresponding energy will range from 22.2 to 6.8 MW. In the same way, the regeneration heat duty will range from 9.9 to 43 MW if the CO₂ concentration in the natural gas is increased from 4 to 10 mol-%.

Table 2. Main characteristics of the heat sources and utilization.

	Unit	Type	Initial T °C	Target T °C	Energy MW
Exhaust gas from turbine	Comp.	Hot	502–550	to atm.	6.8–22.2
Compressed natural gas	Comp.	Hot	131–166	55	2.8–19.0
Lean amine cooler	Sweet.	Hot	57–92	55	0.1–26.7
Amine reg. condenser	Sweet.	Hot	89–95	55	1.8–11.3
Amine reg. reboiler	Sweet.	Cold	128	128	9.9–43.0

3. Heat Integration Model

The proposed integration scheme consists of two parts, as shown in Figure 2: a primary direct heat integration loop that recycles waste heat to the background process and a secondary ORC loop for power production. A grand composite curve of the integrated system is presented in Figure 3, where the main heat integration possibilities have been reported. The overall solution procedure presented in Figure 4 was followed to assess the potential of heat integration for each scenario. The assumptions and solutions methodology of the first loop will be presented in Section 3.1, whereas Section 3.2 will discuss the assumptions of the second loop. Finally, the optimization of the second loop is explained in more detail in Section 3.3.

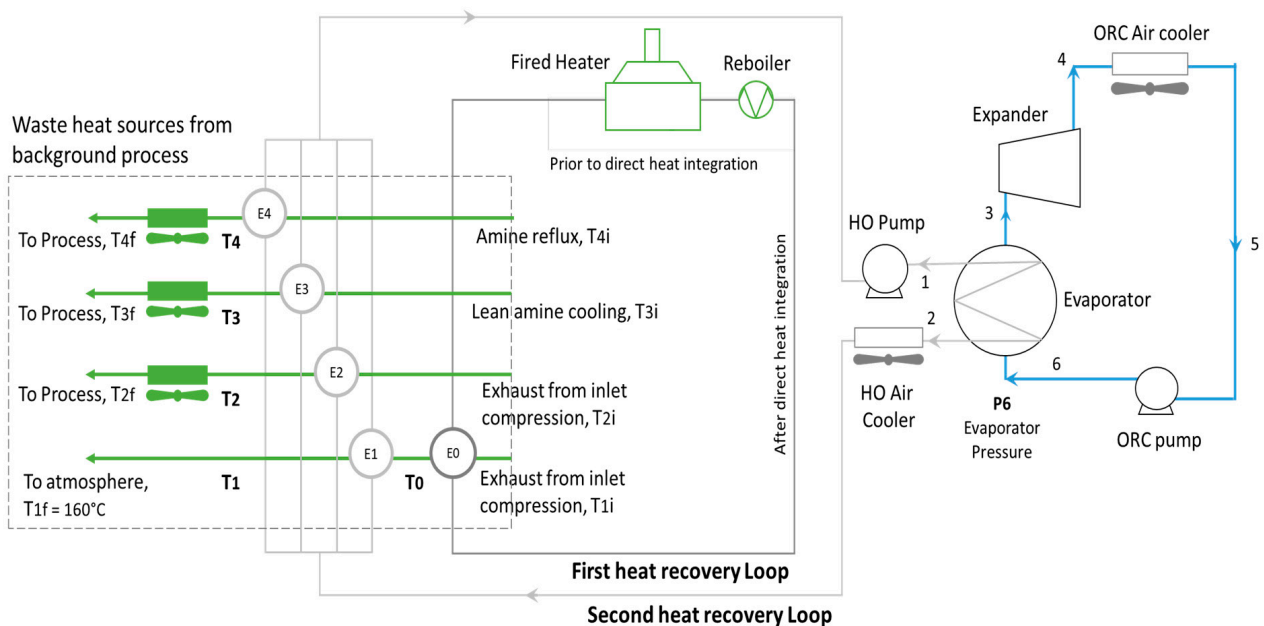


Figure 2. Flowsheet representation of the heat integration scheme.

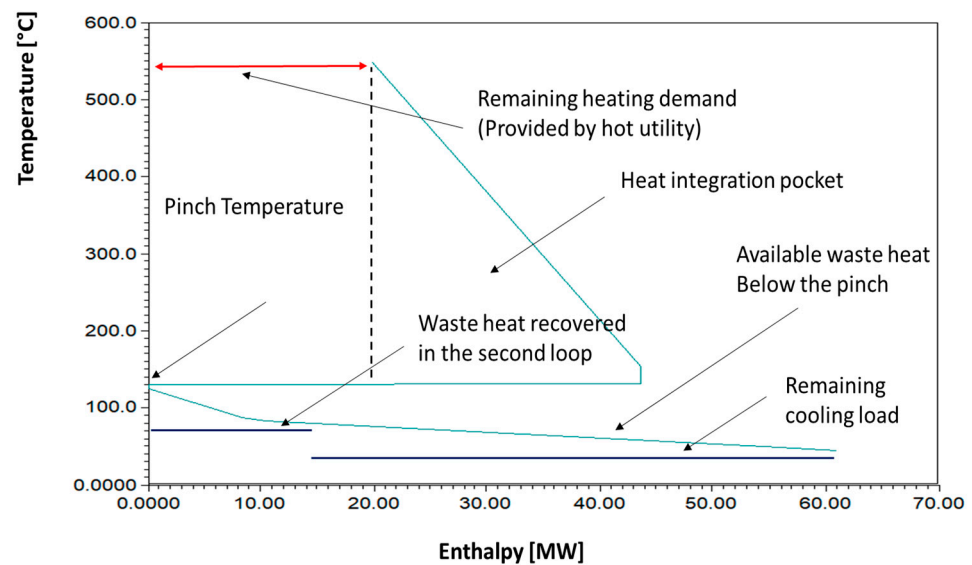


Figure 3. Grand composite curve of the integrated process at 30 bar and 10 mol-% CO₂.

3.1. First Loop: Direct Heat Integration

Before heat integration, the required heat of the sweetening reboiler was completely provided by a fired heater (i.e., external heating source). In order to alleviate fuel consumption, a direct heat integration loop was first added to recycle the waste heat that is available above the pinch.

It should be noted that only the turbine exhaust was found to be at a temperature higher than the pinch point, and thus, it was the only source considered for direct heat integration. The energy balance of the first waste heat recovery exchanger from the turbine's exhaust, noted E0 in Figure 2, was solved by manipulating the outlet temperature of the exhaust, noted T0 in Figure 2, to maximize the heat recovery under three constraints:

- An overall minimum temperature approach of 10 °C;
- A minimum temperature of 160 °C assumed as a cooling limit of the exhausts in order to prevent sulfur condensation;
- A maximal temperature for the heating oil of 177 °C to prevent amine degradation at the skin of reboiler tubes.

3.2. Second Loop: ORC Integration

The application of the organic Rankine cycle for secondary waste heat recovery has been proven to be a reliable method for electricity production from mid- to low-temperature heat sources, such as geothermal, solar, or even waste heat from industrial plants [6]. The ORC system considered in this study uses high-temperature waste heat remaining from direct integration, if available, as well as low-temperature waste heat from the background process.

A basic ORC layout was adopted in this study consisting of an evaporator, a turbine, an air-cooled condenser, and a pump. Table 3 summarizes the assumptions of the ORC loop. The model was built using AspenHysys V11 in order to harness its large thermodynamic properties databank; it was then connected with Matlab (r2020b) through the actxserver command to facilitate the automation of scenarios. The evaporator and condenser were modeled using the weighted heat transfer calculation mode available on AspenHysys, which takes into account the phase change occurring within these units [20]. A saturated vapor was assumed at the inlet of the ORC turbine, and a saturated liquid was assumed at the inlet of the ORC pump. The evaporator pressure was directly optimized by the particle swarm optimization algorithm (PSO), whereas its temperature was indirectly optimized by

manipulating the amount of energy that is absorbed by each heat exchanger of the heat recovery network.

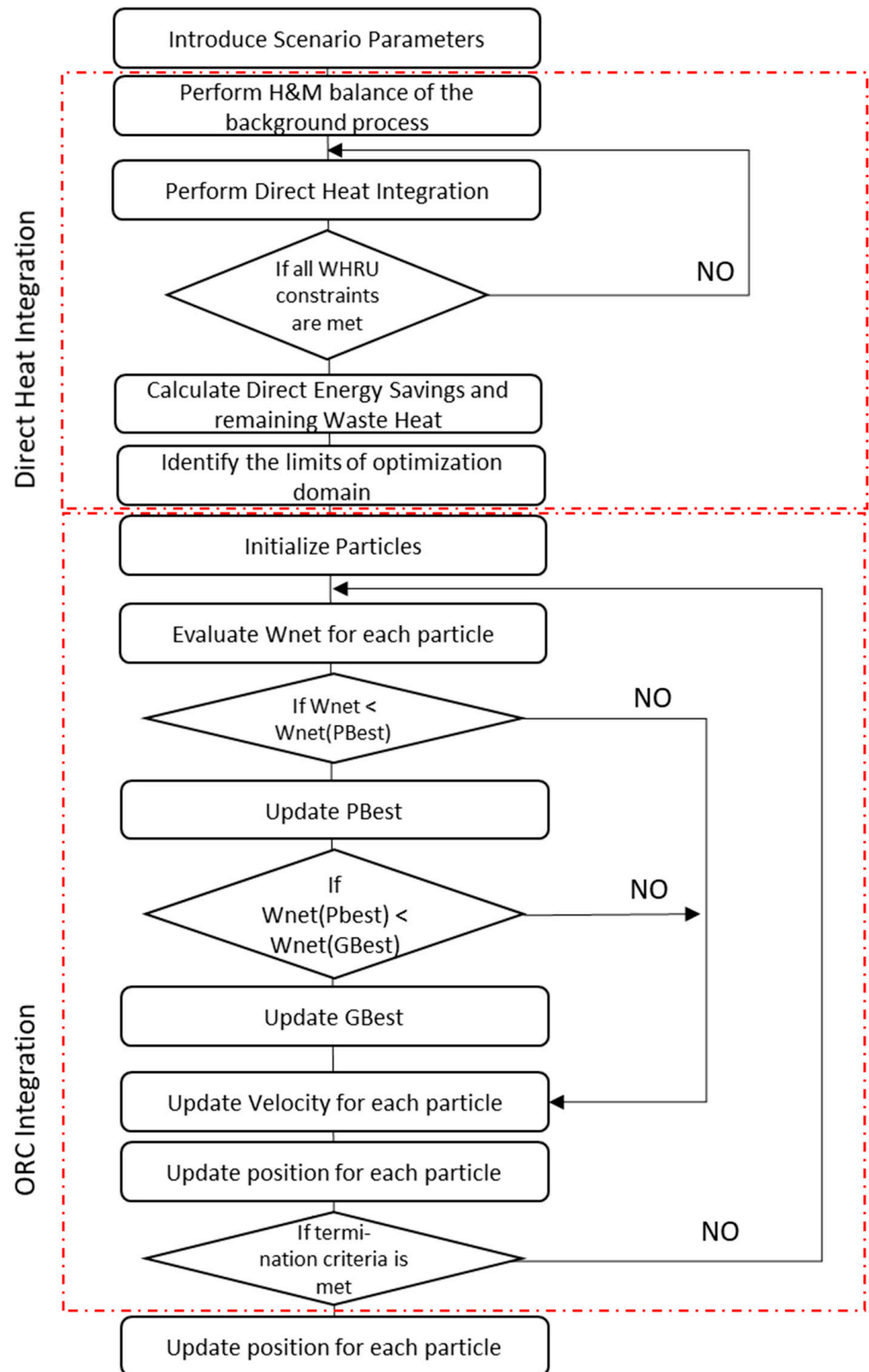


Figure 4. The proposed bi-level heat integration algorithm.

Table 3. Main assumptions of ORC model.

Property Package	Peng-Robinson
Evaporator/Condenser calculation mode	Weighted
Evaporator pressure drop (Hot/Cold)	0.1 bar/0.2 bar
Air condenser pressure drop	0.2 bar
Ambient air temperature	30 °C
Minimum temperature approach	5 °C
Pump efficiency	80%
Expander isentropic efficiency	75%
Total ΔP in the heating oil system	3 bar

The selection of appropriate working fluid is crucial for efficient energy conversion in ORC systems. Additionally, environmental considerations need to be taken into account as many fluids are phased out due to their high ozone depletion potential. In this study, the temperature difference between the heat sources and sink allows many fluids to be used. Yet, as the background process is a natural gas production facility, linear hydrocarbons present a double advantage: an abundant presence in the processed gas and a low environmental impact. This study was limited, however, to the fluids operating above atmospheric pressure. Three candidates found to satisfy these conditions, namely propane (R290), i-butane (R600a), and i-pentane (R601a), were screened all over the investigated domain.

3.3. Optimization Methodology of the Second Loop

The optimization problem was formulated in a way that takes into account the importance of synergy between ORC and the heat recovery network as a unified integrated functioning system. Performing a global optimization on both systems leads to the simultaneous identification of the optimal recovery temperature of each heat exchanger as well as the ORC working pressure corresponding to the highest energy output. Due to the simplicity of its implementation and reported efficiency in solving global optimization problems [21], a particle swarm algorithm (PSO) was used in this study.

PSO is a nature-inspired evolutionary algorithm [22]. It has been successfully applied to solve many engineering problems including the optimization of ORC working parameters [23–25]. In PSO, the possible solutions are represented by a swarm of particles that have their own positions in the search space and which converge to the optimal solution with an individual velocity vector. After each iteration, each particle harnesses its own experience as well as the collective experience of the swarm in order to update its velocity and position as shown in Equations (1) and (2).

$$v_j^{i+1} = w_j v_j^i + c_1 * r_1 (p_{best}^i - x_j^i) + c_2 * r_2 (g_{best}^i - x_j^i) \quad (1)$$

$$x_j^{i+1} = x_j^i + v_j^{i+1} \quad (2)$$

x_j^i , v_j^i in Equations (1) and (2) denote the position and velocity vectors of the particle j at the i th iteration. W_j is the inertia weight that maintains the particle j in its previous direction. c_1 and c_2 are self-adjustment and social adjustment weights that accelerate the particles toward individual best (p_{best}) and global best (g_{best}) positions. r_1 and r_2 are randomly distributed factors in the range of [0, 1] [25]. In this study, a swarm size of 30 particles and self- and social adjustment factors of 0.99 and 1.99, respectively, were used [25]. Moreover, a maximum iteration count of 50 was selected in order to ensure the convergence of the model in an acceptable time, although it was found, as presented in Figure 5, that the PSO algorithm was able to reach the optimum in 20–30 iterations.

Using all the available low-temperature waste heat hinders the performance of the ORC by limiting the application range to low evaporation temperatures only; thus, in addition to the ORC working pressure, the decision variables of the particle swarm algorithm were extended to include the amount of heat absorbed from each of the waste heat sources

listed in Table 2. This was performed by manipulating the outlet temperature of waste heat streams from the heat recovery exchangers. Initial air coolers were maintained to ensure trim cooling so that all streams reach the target process temperature.

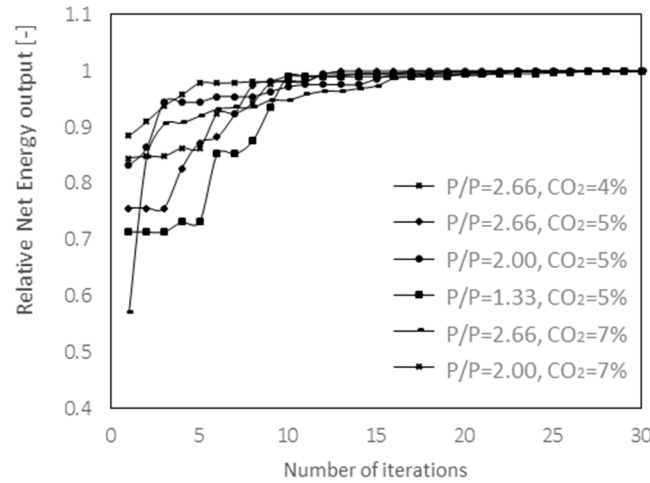


Figure 5. Evolution of fitness function with number of iterations for a sample of scenario.

In this study, the net energy output of the ORC was chosen as the objective function to be maximized. It is the gross power produced by the ORC substituting the pumping energy required to circulate the ORC fluid and the heat transfer fluid for direct heat integration. The decision variables associated with the objective function are the evaporator pressure, noted P6 in Figure 2, and the outlet temperature of the hot streams of the four exchangers, noted T1 to T4 in Figure 2. Evaporator pressure (P6) was set to vary from the pressure upstream of the pump and the critical pressure of the ORC working fluid. The outlet temperature of the heat exchangers (T1 to T4) was set to vary between the initial and target temperatures of the waste heat source ($T_{xf} < T_x < T_{xi}$, $x = 1$ to 4).

The system is subject to other simplification constraints: (i) the investigation is limited to subcritical conditions, and the evaporator temperature is lower than the critical temperature of the chosen fluid. (ii) The saturated vapor and saturated liquid states are assumed at the ORC turbine inlet and pump outlet, respectively. The optimization problem is hence presented as follows:

$$maxNet_Power(\bar{x}) = min. - (W_{ORC} - W_{pump}^{ORC} - W_{pump}^{HO}) \tag{3}$$

With \bar{x} representing the decision variables, which have a range of:

$$P_5 < P_6 < P^{critic} \tag{4}$$

$$T_i^{inlet} \leq T_i \leq T_i^{target}, \quad i = \{1 : 4\} \tag{5}$$

In addition, the system was subject to the following constraints:

$$vf_3 = 1; \quad vf_5 = 0 \tag{6}$$

$$T_5 = T_{amb} + \Delta T_{min} \tag{7}$$

4. Results and Discussion

4.1. Mapping Waste Heat

A mapping of waste heat quantity and quality generated by the sources is presented in Figure 6, where both the total quantity and quality of waste heat over the range of conditions were considered in this study, i.e., CO₂ content in natural gas ranging from

4 to 10 mol-% and an inlet compression ratio ranging from 1.33 to 2.66. The quality of waste heat was calculated by multiplying the energy ratio of each waste heat source by its temperature.

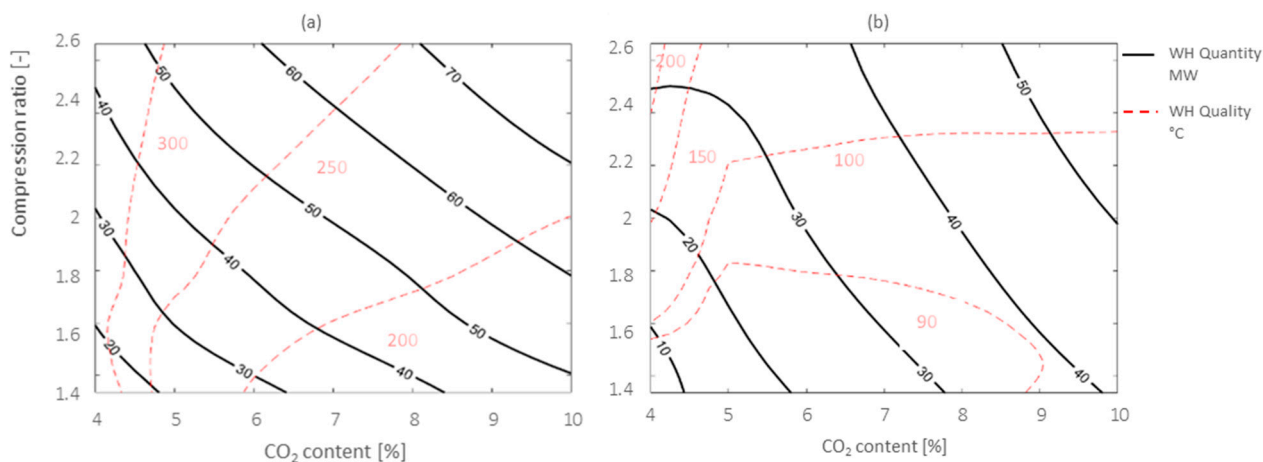


Figure 6. Mapping of waste heat quantity and quality before (a) and after integration (b).

The results show an important potential of waste energy that can be harnessed to improve the efficiency of the background process. However, they also reveal its sensitivity to process conditions, as the available waste heat was found to vary from 20 to 77 MW. This sensitivity can be explained by the fact that the amount of waste heat rejected by the compression unit is proportional to the compression ratio given that the compression efficiency is almost constant. In a similar way, for the amine sweetening unit, the amount of available waste heat increases along with the amine circulation rate and, hence, with the CO₂ content of natural gas feed since feed NG flow and CO₂ specifications were kept constant at 10 MMSCM per day and 2 mol-%, respectively. Consequently, as Figure 6 shows, the lowest waste heat potential is reported at low-pressure-ratio and low-CO₂-content regions, whereas the highest waste heat potential is reported at high-pressure-ratio and high-CO₂-content regions.

4.2. Direct Heat Integration

Waste heat from turbine exhaust presents a high potential for direct energy integration, which may result in a substantial decrease in the amine unit's heating requirement as shown in Figure 7. Results indicate that direct heat integration leads to energy savings ranging from 8 to 20 MW, equivalent to 20 up to 100% of the initial requirements of the amine unit. In addition to the OPEX and environmental benefits, and if addressed in the early design phase, the direct integration may contribute to reducing the capital expenditure cost by reducing the size or even eliminating the external heating source, leading to further cost optimization. As discussed earlier, the highest energy savings are reported at high CO₂ content and high compression pressure ratios, due to the availability of waste heat from the compression stations combined with the high energy requirements of the amine unit.

4.3. ORC Integration

In contrast to direct energy integration, which was found to lead to considerable savings through all the investigated domains, secondary waste heat recovery exhibited a different behavior. As presented previously in Figure 6, the waste heat quantity and quality remaining after the first step were found to vary, respectively, between 10 and 50 MW and 90 and 120 °C. Consequently, the ORC net energy output varied considerably in the studied domain. The highest ORC performance is achieved at a low CO₂ content and high compression ratio, which is a consequence of the availability of relatively high-quality waste heat from the background process as well as an excess of energy from the first integration.

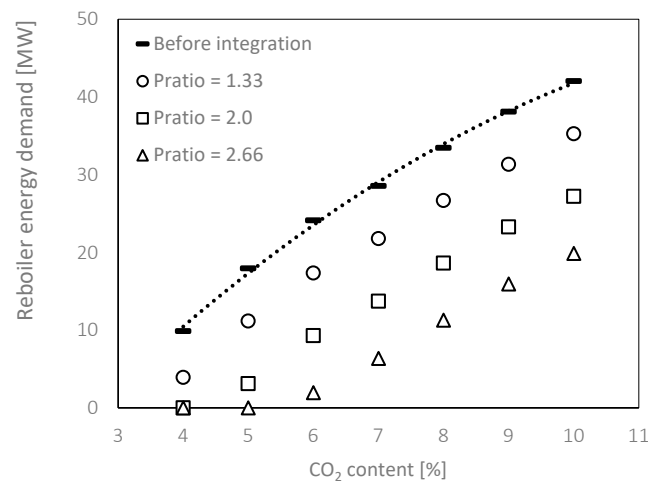


Figure 7. Evolution of heating requirements with CO₂ content before and after first integration at different compression ratios.

In contrast, at a low CO₂ content and low compression ratio, the poor quality of available waste heat drastically reduces the energy conversion efficiency of the ORC system and results in very low power production.

Moreover, the results reveal that the region with larger CO₂ content also presents high potential for secondary waste heat recovery via ORC integration. This feature can be seen in Figure 8, where the ORC net power output increases at CO₂ contents larger than 6% in the case of a pressure ratio of 2.66. In these conditions, due to the increase in the amine flow requirement and, by consequence, its waste heat potential, the sweetening process emerges as an additional source of waste heat along with the compressed NG.

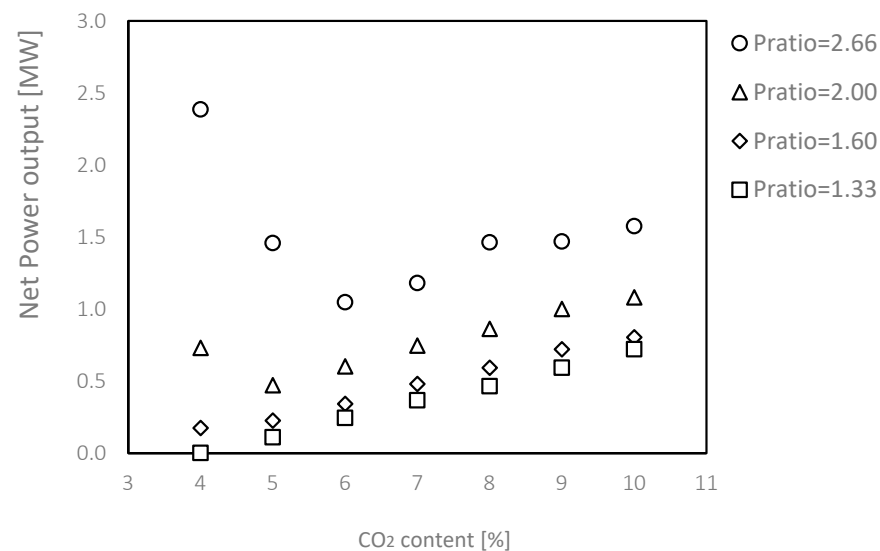


Figure 8. ORC net power output at several conditions using R600a as working fluid.

Figure 9 compares for one specific scenario the contributions of each waste heat source to the ORC power. The same trend was noticed for all other scenarios, where results show that the compression unit is the major contributor at low CO₂ content, whereas the amine unit is the major source of waste heat at high CO₂ content. This is explained by the fact that at higher CO₂ content, all the waste heat from the compression unit is harnessed in direct integration.

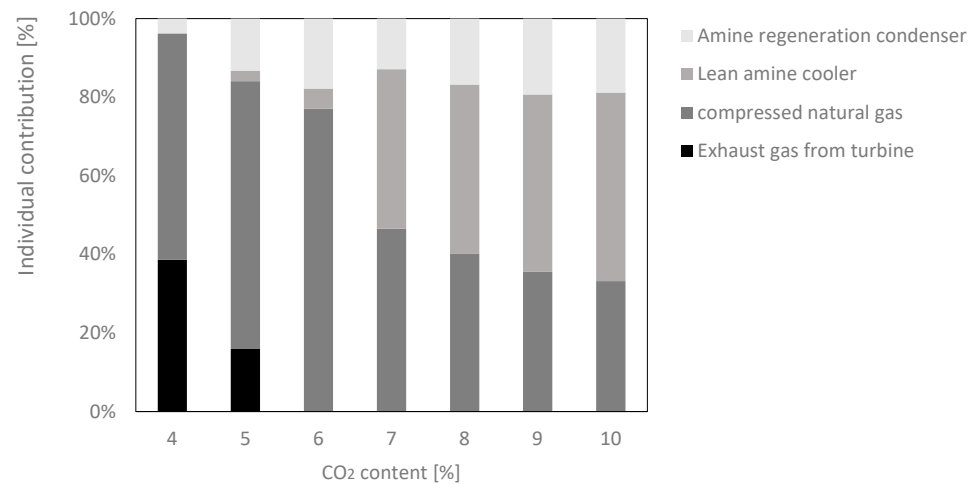


Figure 9. Contribution of individual waste heat sources, Comp. ratio = 2.66, working fluid: R600a.

4.4. Selection of ORC Fluid

The selection of the proper working fluid is of utmost importance for maximal energy output as well as the conversion efficiency of the ORC loop. Moreover, it also impacts the size of the equipment and the working conditions such as the pressure ratio of the turbine, working fluid flow rate, evaporation pressure and temperature, and heat exchanger area. In this study, three different subcritical linear hydrocarbons were screened across the conditions investigated, and the most promising working fluid was identified for each scenario. Figure 10 depicts the behavior of ORC net energy output for the three investigated fluids at different inlet CO₂ content and a compression ratio of 2.66.

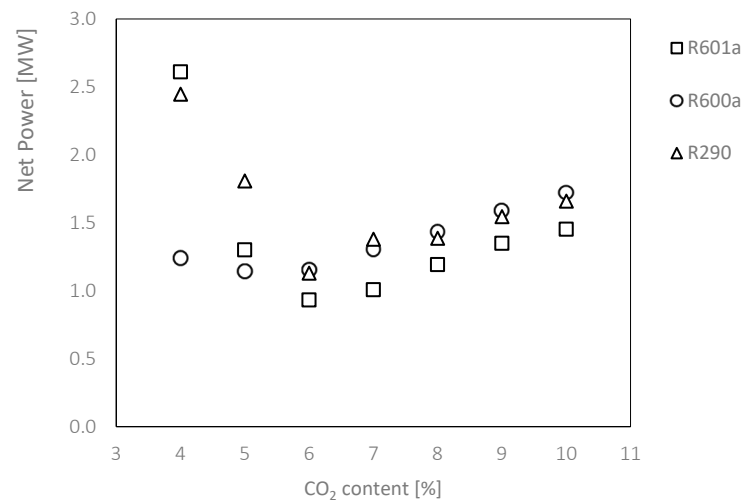


Figure 10. ORC net power output of the different fluids at comp. ratio = 2.66.

In the case of linear hydrocarbons, as the carbon number increases, the results show that the averaged ORC net power between all the scenarios drops by ~8% per carbon number. R290 (propane) was found to outperform other fluids from an energy production standpoint. However, our results also indicate that the required evaporator pressure and flow rate decrease drastically if higher carbon number fluids are used. Moreover, the expansion of propane is wet, meaning that propane droplets can appear at the final stage of expansion, which could be a source of damage if certain types of compressors are used.

In conclusion, even if R290 leads to a slightly improves net power production, higher carbon number fluids are associated with fewer technical challenges, leading to a better trade-off between power production and working conditions. Regarding ORC fluid circula-

tion, the average results of the three working fluids are presented in Table 4. The results indicate that R290 requires a higher flow rate and more pumping power. It is therefore the most sensitive to pump efficiency. The maximum ORC power output associated with the best working fluid suitable for each individual scenario is presented in Figure 11.

Table 4. Averaged ORC results of all scenarios at optimal conditions.

	Unit	R290	R600a	R601a
Evaporator pressure	kPa	2506 ± 32%	1007 ± 53%	400 ± 145%
Net power	kW	872 ± 64%	839 ± 75%	743 ± 71%
Efficiency	%	4.55 ± 36%	4.56 ± 43%	4.55 ± 58%
Flow rate	m ³ /h	389 ± 40%	305 ± 43%	231 ± 40%
Pumping power	kW	376 ± 52%	232 ± 47%	177 ± 35%

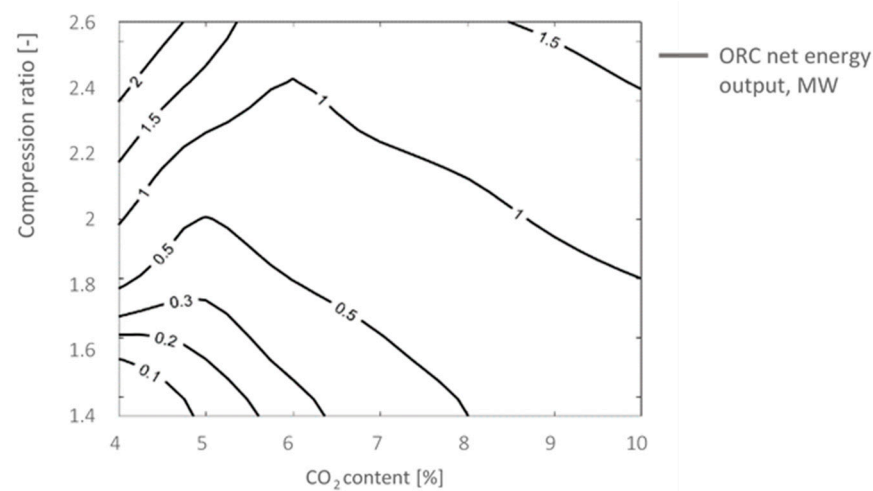


Figure 11. Mapping of ORC net power output all across the investigated domains.

5. Off-Design Performance Analysis

In a natural gas processing plant, the variation of inlet conditions and the simultaneous actions of several controllers induce fluctuations in the heat sources used to power the heat recovery system proposed in this study, which lead to instabilities that affect its efficiency and result in a deviation from the expected nominal performance. For a more realistic assessment of the behavior of the proposed heat integration solution, an off-design analysis was conducted, taking into account real-time temperature and flow rate fluctuations of all the waste heat sources as well as the ambient temperature.

In this regard, real-time data from a natural gas processing plant operated by Sonatrach were extracted at a 50 min interval over 31 days of stable operations. The signals were used to create a perturbation around the conditions of a steady-state scenario. The scenario with 7% CO₂ and 2.66 compression ratio was selected, as it was the closest to the conditions of the real plant. Table 5 summarizes the characteristics of the fluctuating input signals. For the three working fluids, the optimized design parameters of the heat integration scheme were maintained and the model was then evaluated at each point.

The off-design analysis was conducted under the following assumptions:

- The heat transfer area (UA) of each heat exchanger obtained using design conditions was maintained in the off-design analysis.
- The pump was assumed to deliver the required flow rate and outlet pressure at the design efficiency—an acceptable assumption given that the ORC fluid flow rate was found to range within ±10% of the design value.
- The turbine was also assumed capable of delivering the expansion ratios despite the fluctuating conditions. However, due to the large deviation in expander energy output

of $\pm 30\%$, the efficiency of the turbine was corrected using Equation (8) [26], where θ represents the efficiency and the “on” and “off” indices indicate, respectively, the design and off-design values of a parameter.

$$\theta_{off} = \theta_{on} \sin \left[0.5 * \pi \left(\frac{\dot{m}_{off} * \rho_{on}}{\dot{m}_{on} * \rho_{off}} \right)^{0.5} \right] \tag{8}$$

Table 5. Characteristics of the fluctuating heat sources and sink.

	Variable	Nominal	Unit	SDV%	Max%	Min%
Exhaust gas from turbine	Flow rate	6437	kmol/h	2.2	103.3	88.9
	Temperature	550	°C	0.36	100.9	98.7
Compressed NG	Flow rate	17,620	kmol/h	1.65	119.6	96.0
	Temperature	131	°C	1.33	104.9	96.5
Lean amine cooler	Flow rate	17,480	kmol/h	0.95	103.9	97.1
	Temperature	87	°C	1.15	109.3	97.0
Amine regeneration condenser	Flow rate	1594	kmol/h	0.95	103.9	97.2
	Temperature	94	°C	1.52	103.4	92.2
Ambient air	Temperature	25	°C	25.2	162.2	53.1

Figure 12 represents the probability distribution of both source and sink temperatures of the ORC system. The heat source temperature varies between 90 and 120% of the nominal value; however, the sink, which is the ambient temperature, shows a bi-modal distribution around 90% and 130% of the design temperature representing, respectively, the average day and night temperatures during the 31 days of data extraction. On the other hand, Figure 13 shows the resulting ORC performance of the three fluids depicted as efficiency versus net energy output.

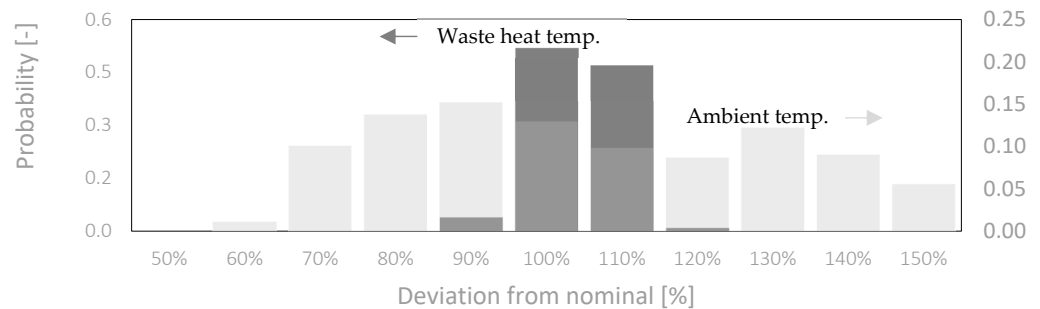


Figure 12. Temperature distribution of heat source and ambient temperature.

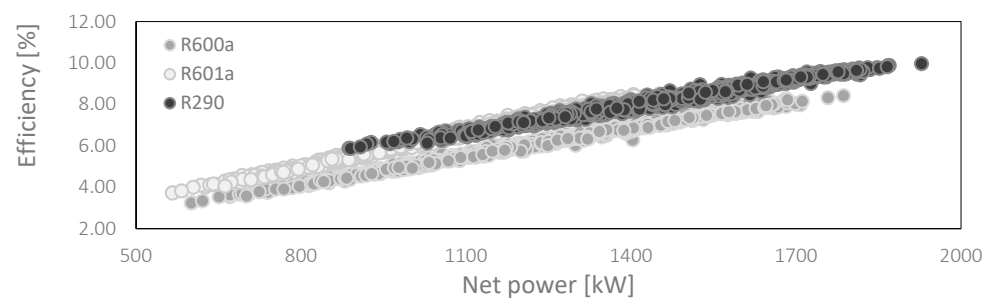


Figure 13. ORC performance in off-design conditions.

Off-design analysis results, presented in Figure 14, indicate that energy savings from the first integration present a narrow variation around the nominal value, which is due to

their exclusive dependence on the waste heat from the turbine exhaust. On another hand, the profile of ORC net power output of all fluids presents a wider bi-modal distribution. This behavior is due to its dependence on several waste heat sources as well as the ambient temperature. The results also show that each fluid performs at a different efficiency and demonstrates a different sensitivity to the same changes in inlet conditions. R290 showed the highest efficiency and the narrowest variation around the nominal point. Efficiency results are depicted in Figure 13.

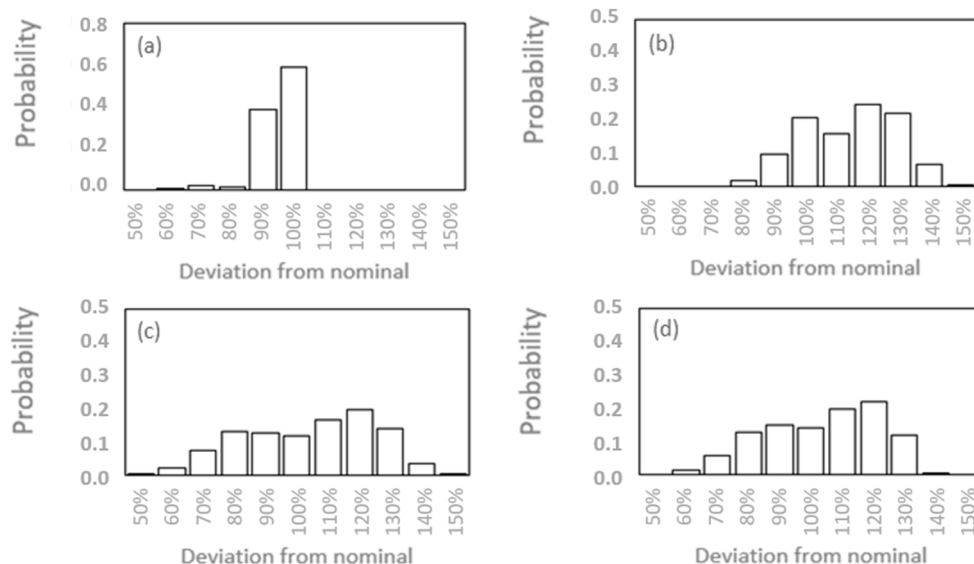


Figure 14. Distribution of energy output, (a) Energy savings from direct heat integration, (b) Net energy output (R290), (c) Net energy output (R600a), and (d) Net energy output (R601a).

6. Conclusions

This study investigates the use of waste heat as a means to increase the energy efficiency of sweetening units in the context of natural gas upstream processing. Carbon capture in natural gas processing plants could lead to significant emission reductions in the case that the captured CO₂ is stored or re-used, but its impact on the energy balance of the process is significant. A heat integration scheme consisting of two steps was proposed to address this issue. Firstly, the direct integration of high-temperature waste heat is proposed, and secondly, the use of ORC is used as a bottoming cycle technology. The following conclusions were drawn:

Direct heat integration of inlet natural gas compression units with the amine sweetening unit leads to considerable energy savings ranging from 8 to 20 MW, which is equivalent to 20 to 100% of the thermal requirements of the amine unit. The highest integration potential was met at low CO₂ content, where the energy demand of the process is low compared to the available amount of waste heat. Such integration results in a net improvement of energy and environmental performances of the background process. Moreover, if performed in the early design stages, it contributes to cutting CAPEX down by reducing the size of the external heating equipment.

ORC integration for secondary waste heat was feasible in most of the investigated domains. However, the net energy output was found to be highly sensitive to process conditions. Its value ranges from 100 up to 2600 kW. The results show that the most favorable conditions for ORC integration are a CO₂ content lower than 5% and a compression ratio larger than 2. The results also showed that for a CO₂ content lower than 4% and compression ratios smaller than 1.6, the waste heat quality was not high enough to ensure the evaporation of the selected fluids. From a net energy output point of view, R290 was found to outperform R600a and R601a in most scenarios. Yet, it requires a much higher

evaporator pressure and fluid flow rate along with engineering challenges associated with its wet expansion. A net power output of 2.6 MW could be achieved in some conditions.

Finally, the off-design analysis offered a better potential assessment of the proposed solution through quantification of the impact of temperature fluctuations of waste heat sources and sinks. A deviation of ± 68 to $\pm 103\%$ around the nominal energy savings was found for the direct heat integration, and deviations from the nominal net ORC power output were sensitive to the working fluid. They ranged from 60 to 132% for R290, from 47 to 142% for R600a, and between 52 and 135% for R601a.

This work reveals that ORC can play an important role as a waste heat recovery technology. In future work, we will extend the concept developed in this study to include high-temperature heat pumps, which are emerging as a promising technology for industrial decarbonization.

Author Contributions: Conceptualization, A.B.; Methodology, A.B.; Validation, S.B. and G.L.; Data curation, A.B. and M.G.; Writing—original draft, A.B.; Writing—review & editing, M.G. and G.L.; Supervision, G.L. All authors have read and agreed to the published version of the manuscript.

Funding: The authors are grateful to the Belgian Federal Public Service, who partially supported M. A. Berchiche through the Energy Transition Fund and the Procura project.

Data Availability Statement: The industrial data presented in this study are available on request from the corresponding author.

Conflicts of Interest: The authors declare no conflict of interest.

References

1. IEA. *World Energy Outlook 2021*; IEA: Paris, France, 2021.
2. British Petroleum. *Statistical Review of World Energy 2021*; British Petroleum: London, UK, 2021.
3. Hung, T.C.; Shai, T.; Wang, S.K. A review of organic Rankine cycles (ORCs). *Energy* **1997**, *22*, 661–667. [[CrossRef](#)]
4. Su, Z.; Zhang, M.; Xu, P.; Zhao, Z.; Wang, Z.; Huang, H.; Ouyang, T. Opportunities and strategies for multigrade waste heat utilization in various industries: A recent review. *Energy Conv. Manag.* **2021**, *229*, 113769. [[CrossRef](#)]
5. Siyao, L.; Jie, H.; Dexiang, L. Optimal integration of methanol-to-gasoline process with organic Rankine cycle. *Chem. Eng. Res. Des.* **2020**, *154*, 182–191.
6. Tartière, T.; Astolfi, M. A World Overview of the ORC Market. In Proceedings of the IV International Seminar on ORC Power Systems, Milano, Italy, 13–15 September 2017; pp. 13–15.
7. Shaikh, A.Z.; Alnouss, A.; Al-Ansari, T. A heat integration case study for the dehydration and condensate stabilization units in LNG plants for economic and energy savings. *Comput. Chem. Eng.* **2022**, *168*, 108062. [[CrossRef](#)]
8. Zhang, Y.; Wang, B.; Liang, Y.; Yuan, M.; Varbanov, P.S.; Klemes, J.J. A method for simultaneous retrofit of heat exchanger networks and tower operations for an existing natural gas purification process. *Adv. Electr. Eng. Electron. Energy* **2021**, *1*, 100019. [[CrossRef](#)]
9. Yu, H.; Feng, X.; Wang, Y.; Biegler, L.; Eason, J. A systematic method to customize an efficient organic Rankine cycle to recover waste heat in refineries. *Appl. Energy* **2016**, *179*, 302–315. [[CrossRef](#)]
10. Veloso, T.G.C.; Sotomonte, C.A.R.; Coronado, C.J.R.; Nascimento, M.A.R. Multi-objective optimization and exergetic analysis of a low-grade waste heat recovery ORC application on a Brazilian FPSO. *Energy Conv. Manag.* **2018**, *174*, 537–551. [[CrossRef](#)]
11. Ting, H.; Wensheng, L. Energy saving research of natural gas liquefaction plant based on waste heat utilization of gas turbine exhaust. *Energy Conv. Manag.* **2020**, *225*, 113468.
12. Zhao, H.L.; Dong, H.; Tang, J.; Cai, J. Cold energy utilization of liquefied natural gas for capturing carbon dioxide in the flue gas from the magnesite processing industry. *Energy* **2016**, *105*, 45–56. [[CrossRef](#)]
13. Bianchi, M.; Branchini, L.; De Pascal, A.; Melino, F.; Peretto, A.; Archetti, D.; Campana, F.; Ferrari, T.; Rossetti, N. Feasibility of ORC application in natural gas compressor stations. *Energy* **2019**, *173*, 1–15. [[CrossRef](#)]
14. Leonard, G.; Crosset, C.; Toye, D.; Heyen, G. Influence of process operating conditions on solvent thermal and oxidative degradation in post-combustion CO₂ capture. *Comput. Chem. Eng.* **2015**, *83*, 121–130. [[CrossRef](#)]
15. Nuchitprasittichai, A.; Cremaschi, S. Optimization of CO₂ capture process with aqueous amines using response surface methodology. *Ind. Eng. Chem. Res.* **2013**, *52*, 10236–10243. [[CrossRef](#)]
16. Peters, L.; Hussain, A.; Follman, M.; Melin, T.; Hagg, M.B. CO₂ removal from natural gas by employing amine absorption and membrane technology—A technical and economical analysis. *Chem. Eng. J.* **2011**, *172*, 952–960. [[CrossRef](#)]
17. Peng, D.Y.; Robinson, D.B. A New Two-Constant 18 Equation of State. *Ind. Eng. Chem. Fundam.* **1976**, *15*, 59–64. [[CrossRef](#)]
18. Siemens Gas Turbine Portfolio 2018, Article-No. PGDG-B10006-04-4A00. Available online: www.siemens.com (accessed on 21 September 2020).

19. Li, Y.; Mather, A.E. Correlation of the Solubility of CO₂ in a Mixed Solution. *Ind. Eng. Chem. Res.* **1994**, *33*, 2006–2015. [[CrossRef](#)]
20. Kamaruddin, A. *Aspen HYSYS: An Introduction to Chemical Engineering Simulation*; Lambert Academic Publish: London, UK, 2013.
21. Javaloyes-Anton, J.; Ruiz-Femenia, R.; Caballero, J.A. Rigorous design of complex distillation columns using process simulators and the particle swarm optimization algorithm. *Ind. Eng. Chem. Res.* **2013**, *52*, 15621–15634. [[CrossRef](#)]
22. Kennedy, J.; Eberhart, R. Particle swarm optimization. In Proceedings of the ICNN'95-international conference on neural networks, Perth, Australia, 27 November–1 December 1995; pp. 1942–1945.
23. Grag, P.; Orosz, M.S. Economic optimization of Organic Rankine cycle with pure fluids and mixtures for waste heat and solar applications using particle swarm optimization method. *Energy Conv. Manag.* **2018**, *165*, 649–668. [[CrossRef](#)]
24. Rui, Z.; Hongguang, Z.; Songsong, S.; Fubin, Y.; Xiaochen, H.; Yuxin, Y. Global optimization of the diesel engine–Organic Rankine cycle (ORC) combined system based on particle swarm optimizer (PSO). *Energy Conv. Manag.* **2018**, *174*, 248–259.
25. Kyungtae, P.; Soung-Ryong, O.; Wangyun, W. Techno-economic optimization of the integration of an organic Rankine cycle into a molten carbonate fuel cell power plant. *Korean J. Chem. Eng.* **2019**, *36*, 345–355.
26. In, S.K.; Tong, S.K.; Jong, J.L. Off-design performance analysis of organic Rankine cycle using real operation data from a heat source plant. *Energy Conv. Manag.* **2017**, *133*, 284–291.

Disclaimer/Publisher's Note: The statements, opinions and data contained in all publications are solely those of the individual author(s) and contributor(s) and not of MDPI and/or the editor(s). MDPI and/or the editor(s) disclaim responsibility for any injury to people or property resulting from any ideas, methods, instructions or products referred to in the content.